Volume 13, Number 3, 2020. pp. 181-190

Jordan Journal of Physics

ARTICLE

Critical Behavior of Electrical Conductivity for Reduced Graphene Oxide/Epoxy Resin Composites

Y. Nioua[a], S. El Bouazzaoui[a], B. M. G. Melo[b], P. R. Prezas[b], M. E. Achour[a], M. P. F. Graça[b], L. C. Costa[b], A. Fattoum[c] and M. E. Touhami[d]

[a] *Laboratory of Materials Physics and Subatomic, Faculty, University Ibn Tofail, BP 242, 14000, Kenitra, Morocco.*

[b] *I3N and Physics Department, University of Aveiro, 3810-193 Aveiro, Portugal.*

[c] *Research Unit of Materials, Environment and Energy, Sciences Faculty of Gafsa, 2112 Gafsa, Tunisia.*

[d] *Laboratoire d'Ingénierie des Matériaux et d'Environnement: Modélisation et Application, Sciences Faculty, University Ibn Tofail, BP 133, 14000, Kenitra, Morocco.*

Doi : https://doi.org/10.47011/13.3.1

Received on: 08/08/2019; *Accepted on: 5/12/2019*

Abstract: In this paper, we analyze the dc and ac electrical conductivities, in the 240 to 400 K temperature range and 10^2 to 10^6 Hz frequency range, of a percolating system synthesized by mixing reduced graphene oxide (rGO) particles in insulating epoxy resin matrix, diglycidyl ether of bisphenol A (DGEBA). We found that the dc electrical conductivity of the samples is strongly related to the rGO content, indicating a percolating behavior with percolation threshold $\phi_C \approx 4$ %. The critical behavior of the dc electrical conductivity as a function of the temperature indicates a strong positive temperature coefficient and a negative temperature coefficient of resistivity below and above the transition temperature T_g, respectively. Moreover, the results showed that the dc conductivity obeys the Arrhenius law and the ac electrical conductivity is both frequency and temperature dependent and follows the Jonscher's power law.

Keywords: Composites, Dielectric properties, Fillers, Glass transition, Graphene.

Introduction

Electrically conductive polymer composite materials, formed by inserting conductive particles, such as graphite, carbon black (CB), carbon nanotubes (CNTs), … etc., into an insulating polymer matrix, are considered to be an important group of multifunctional materials for many potential engineering applications [1-3]. Since its discovery by Geim's group in 2004 [4], graphene (GE) has proven to be better than other carbonaceous materials concerning many unique properties, such as very large Young's modulus (≈ 1 TPa) and fracture strength (≈ 130 GPa), high thermal conductivity (≈ 5000 W/ mK), high electrical conductivity (≈ 6000 S/cm) and high surface area (≈ 2600 m^2/g) [5]. These properties attracted great interest in the modern electronics and electrical engineering fields and provide graphene the potential to enhance electronic devices, sensors, energy storage systems, potential battery cells and biomedical applications [6-7]. Recently, extensive investigation has been focused on the exploration of the graphene-based materials properties for the fabrication of nanocomposites

Corresponding Author: M. E. Achour **Email**: achour.me@univ-ibntofail.ac.ma

with different polymer matrices [8], on the description of the synthesis methodologies of these nanocomposites and on the characterization of their mechanical properties [9]. However, there is a scarce amount of reports addressing the electrical and dielectric properties of polymer/graphene composite materials. In our previous work [10], we presented the impedance spectroscopy analysis of composite materials, fabricated by mixing reduced graphene oxide (rGO) in an epoxy resin, over a broad frequency and temperature range.

In the present work, our primary interest is to analyze the dc and ac electrical conductivities of epoxy resin polymer loaded with rGO particles, in the 240 to 400 K temperature range over the 10^2 up to 10^6 Hz frequency range. Secondly, we focus our interest on the analysis of the positive temperature coefficient (PTCR) [11-13] and negative temperature coefficient (NTCR) [14] effects which are observed on the electrical measurements, at temperatures below and above the glass transition temperature (Tg). Furthermore, we used some theoretical models dealing with the charge transport mechanisms in disordered materials to fit the experimental results.

Experimental

Materials

The samples investigated in this study are reduced graphene oxide (rGO) particles dispersed in an epoxy resin matrix (DGEBA). The rGO was purchased from Graphenea, with an average particle size of about 260-295 nm, the density is 1.91g.cm^{-3} and the specific surface area [15] is between 423 and 500 m^2.g^{-1}. The insulating resin epoxy prepolymer D.E.R. 321 has an epoxy equivalent weight of 180–188 (g/eq), a density of 1.14 g.cm^{-3} at 25 ºC, a viscosity of 500–700 (mPa.s) at 25 °C and a glass transition temperature $T_g \approx 360$ K. Eight samples with 0 (pure polymer), 2, 3, 4, 6, 8, 10 and 14 wt % of rGO were synthesized by mixing the desired volume fraction ϕ with the prepolymer, followed by the curing process. Gelation took 5 minutes for each sample and subsequently, the mixture was poured into a mold. After a few hours, the samples were unmolded and left to rest for about 24 h, in order to complete the polymerization process and to promote the homogeneity of the inclusion distribution in the polymer matrix [10]. The sample morphology of the rGO/epoxy composite materials was analyzed using by scanning electron microscopy SEM (SEM, HITACHI S-3200N).

Electrical Measurements

For the electrical measurements, the samples were prepared as discs with a diameter of 15 mm and a thickness of 2 mm and the electrical contacts were formed by painting both opposite faces with a conductive silver paint. The dc electrical conductivity σ_{dc} measurements were made in a helium atmosphere, in the temperature range from 240 to 400 K using a Keithley 617 programmable electrometer. The temperature dependent alternating current (ac) impedance spectra were measured by using an Agilent 4292A impedance analyzer in the C_P-R_P configuration over broad frequency (100 kHz -1 MHz) and temperature ranges (240-400K). The complex admittance $Y^*(\omega) = 1/Z^*(\omega) = G(\omega) + jB(\omega)$ could be converted into the complex permittivity formalism $\varepsilon^*(\omega) = \varepsilon'(\omega) - j\varepsilon''(\omega)$ using the relations $\varepsilon'(\omega) = B(\omega)e/\varepsilon_0 A\omega$ and $\varepsilon''(\omega) = G(\omega)e/\varepsilon_0 A\omega$, where A is the cross-sectional area of the sample, e is its thickness and ε_0 is the free space permittivity. The terms $G(\omega)$ and $B(\omega)$ are, respectively, the conductance and the susceptance of the samples [16-17]; afterward, the ac electrical conductivity can be calculated using the relation $\sigma_{ac}(\omega) = \omega.\varepsilon_0.\varepsilon''$ [16].

Results and Discussion

Morphological Characteristics

The SEM micrographs of the rGO/epoxy nanocomposites, with rGO concentrations of $\phi = 4.42$ % and $\phi = 6.21$ %, are shown in Fig. 1. The reduced graphene oxide particles are selectively dispersed in the epoxy polymer and with further increase of the rGO gradually, a continuous conductive path forms in the polymer matrix. Both micrographs show rGO clusters due to their tendency to agglomerate in the polymer matrix. Aggregation and overlapping structures are easily formed in the graphene/polymer composites, because the graphene nanoparticles have a large specific surface area (423 – 500 m^2/g) [14].

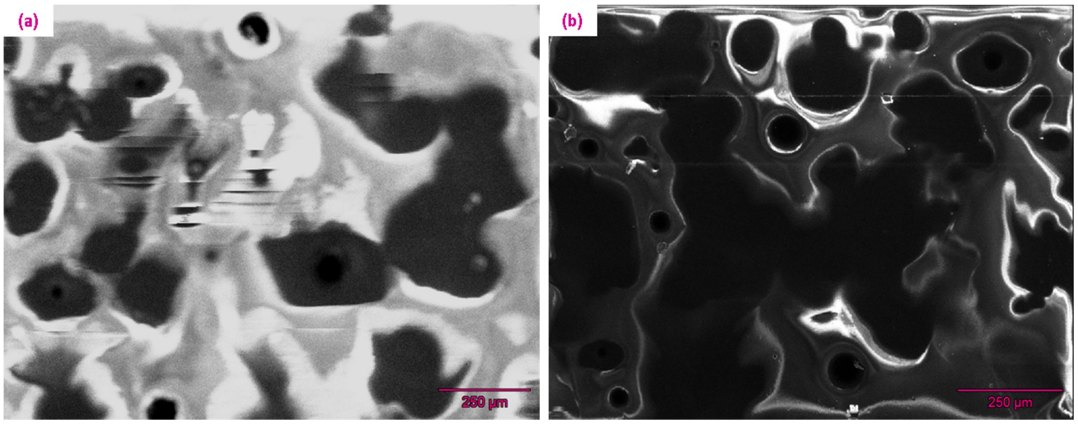

FIG. 1. SEM micrographs of the rGO/epoxy composites with 4.42 % (a) and 6.21 % (b) filler concentrations.

Percolation Threshold

Fig. 2 shows the dc electrical conductivity of the rGO/epoxy composites as a function of the rGO concentration, at room temperature. It is observed that, at very low filler loading, the electrical conductivity is dominated by the insulator polymer matrix and the conductivity values in this range are around 10^{-13} ($S.m^{-1}$), typical of dielectric materials. On the other hand, for higher filler loadings, a sharp increase in the electrical conductivity, over 8 orders of magnitude (from 1.52×10^{-11} S/m for 3.66 % to 1.93×10^{-3} S/m for 4.93 % of rGO), is observed. This abrupt transition indicates the formation of an interconnected rGO network, causing a decrease in the distance that separates the sheets. The percolation threshold is clearly observed and the experimental ϕ_C value was estimated to be around $\approx$ 4 %. The obtained percolation threshold is higher than those of a series of rGO/polymer composites reported by A. J. Marsden et al. [18]. This disagreement may be related to the shape of the conductive particles (rGO) [19], aggregation and overlapping of reduced graphene oxide due to its large specific surface area [20-21], the viscosity of the composite, because the very low percolation thresholds are always achieved with a low viscosity system [22] and could be also a result of the degree of dispersion between rGO particles and the polymer matrix [22].

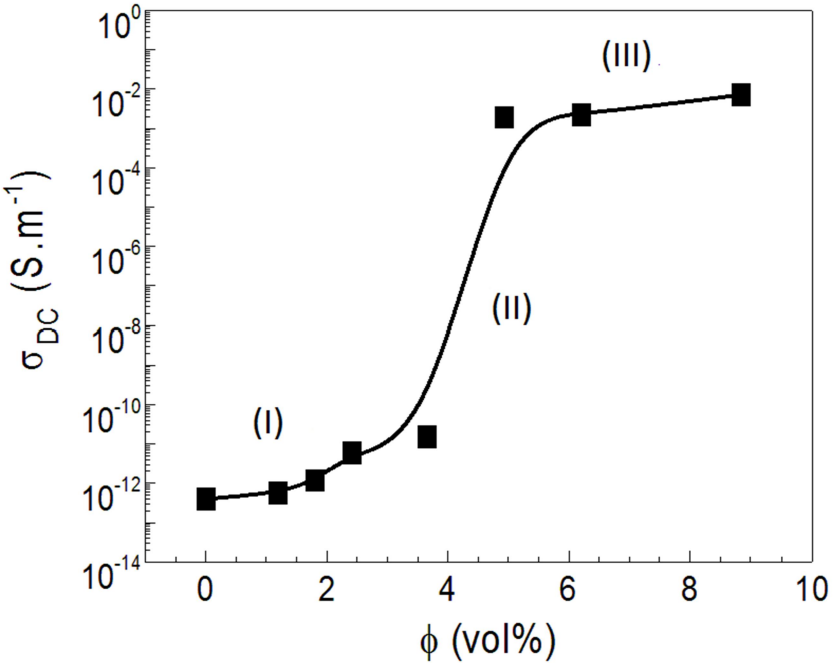

FIG. 2. dc electrical conductivity, σ_{dc} *versus* rGO concentration in the rGO/epoxy composites, at room temperature T= 300 K.

Electrical Resistivity Analysis

The distribution of the conductive particles in a polymer insulating matrix can give rise to electrically conductive polymer composites and some of these materials can exhibit a critical behavior around the glass transition temperature (T_g). Below Tg, some materials show an abrupt increase in resistivity when the temperature changes only over a few degrees. This phenomenon is known as PTCR effect.

Fig. 3 depicts the electrical resistivity ($\rho = 1/\sigma_{dc}$) of the rGO/epoxy composites as a function of temperature, for concentrations above the percolation threshold. In order to analyze and understand the data presented in Fig. 3, it is necessary to consider three regions: (i) from 240 to $T_g \approx 356$ K [10], in which the resistivity decreases with temperature, which is a typical behavior for semiconductors and insulators; (ii) from 356 to 380 K, where the opposite behavior is observed, typical of conductive materials: an increase of the electrical resistivity with temperature, showing a PTCR effect. The mechanism responsible for this behavior may be attributed to the tunneling effect and it can be explained as follows: above a critical temperature (T_g), the epoxy polymer volume expansion is enhanced and the interparticle distance tends to rapidly increase with increasing temperature, causing a sharp increase in the resistivity [12, 23-24]; (iii) Above 380 K, a similar variation occurs as observed in (i). In the latter temperature region, one can see a decrease of the resistivity with increasing temperature, showing the NTCR effect. It is generally accepted that the NTCR effect is attributed to the reaggregation of the conductive fillers and the reformation of the conductive networks [14]. Overall, one can say that the electrical resistivity temperature variation of the composite materials above the threshold filler concentration is consistent with a PTCR effect above the glass transition temperature T_g.

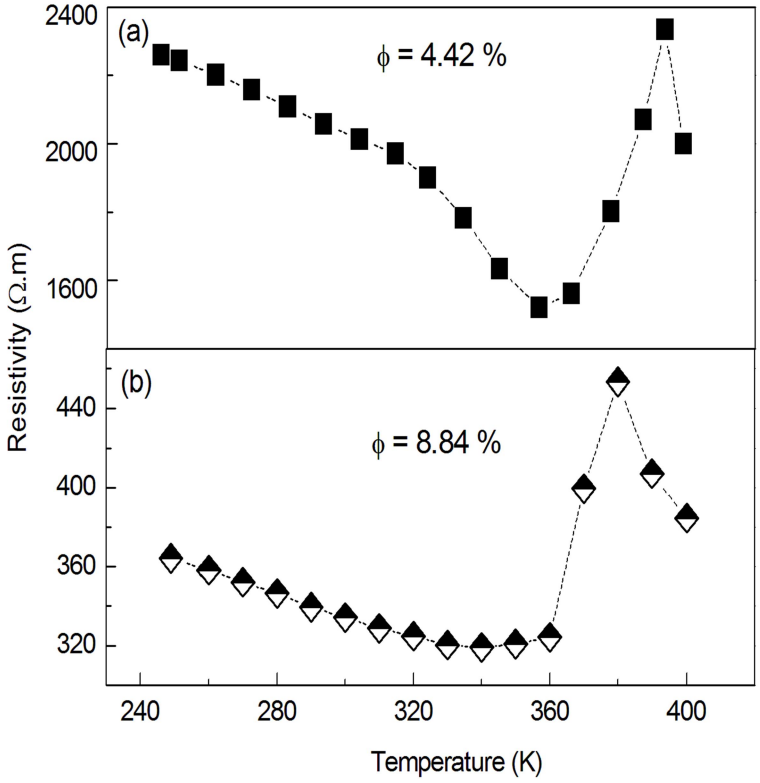

FIG. 3: Temperature dependence of the resistivity of the rGO/epoxy composites, for concentrations above the percolation threshold 4.42 % (a), 6.21% (b) and 8.84 % (c).

For further discussion of the PTCR effect, it is important to consider the PTCR intensity I_{PTC}, defined as the ratio of the maximum resistivity (ρ_{max}) to the resistivity at room temperature (ρ_{RT}), which can be calculated from the temperature dependence of the composite's resistivity, as shown in Eq. (1) [23]:

$$I_{PTC} = \frac{\rho_{max}}{\rho_{RT}}. \quad (1)$$

Fig. 4a shows the PTC intensity of the rGO/epoxy composites as a function of the rGO content, for concentrations above the percolation threshold. As expected, the rGO concentration has a significant influence on the PTC intensity. We see that the highest value is obtained for $\phi \approx 6.21\,\%$, then it decreases with increasing rGO content. Fig. 4b and Fig. 4c show some results of the PTC intensity from other rGO/epoxy composites of our previous works, made from epoxy resin-filled carbon nanotubes (CNTs); namely, CNT/polyester composite (Fig. 4b) [16] and CNT/epoxy composite (Fig. 4c) [25]. These indicate that the I_{PTC} for the rGO/epoxy is relatively high compared to the other polymeric composite materials; this result can be explained by the strong agglomeration of the conductive particles (rGO) in the polymer matrix, because agglomeration may have a strong influence on the PTCR effect of the composite materials [14]. Additionally, we would like to indicate that the increase of resistivity with the increment of the temperature seen in the rGO/epoxy composites has been largely studied and such information is critical for the development of multifunctional polymer composites. A similar study has also been reported by Jun-Wei Zha et al. [26] for CB/MWNT/HDPE and CB/HDPE composites' materials.

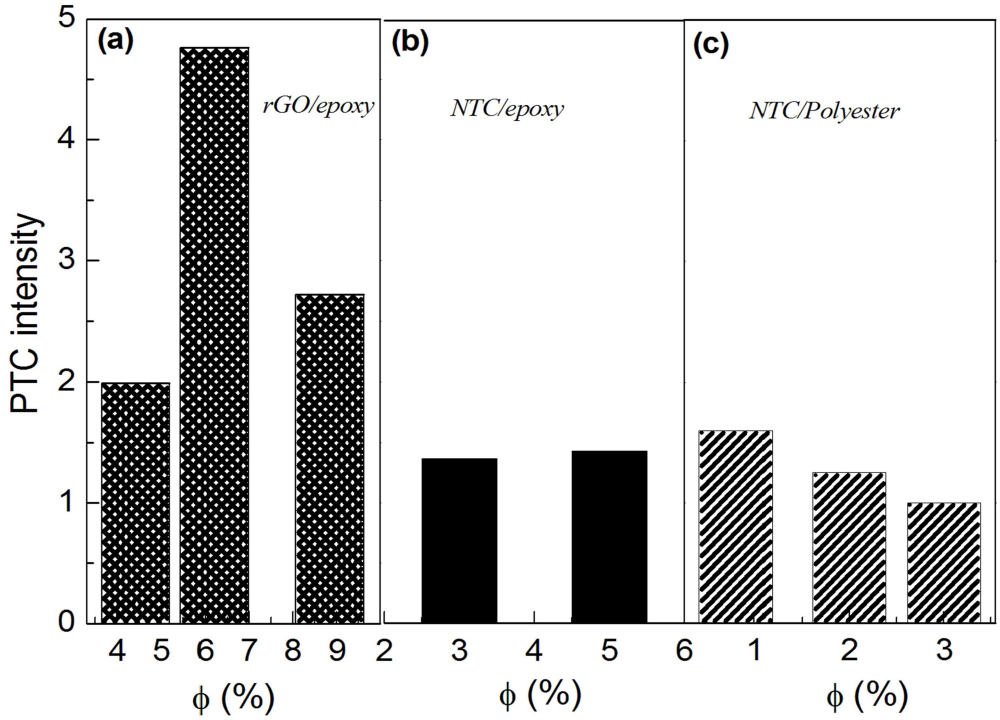

FIG. 4. PTC intensity of the rGO/epoxy composites compared with other systems from our previous works.

AC Electrical Conductivity Analysis

To a better understanding of the frequency and temperature dependence of the electrical properties of the studied samples, ac electrical conductivity measurements were carried out for all samples. Fig. 5 summarizes the ac conductivity as a function of frequency for several temperatures, for a concentration below the percolation threshold (3.66 %). It is visible that at low frequencies, the ac electrical conductivity remains constant, especially for high temperatures; this is attributed to the dc electrical conductivity contribution. At higher frequencies, it becomes strongly frequency and temperature dependent and increases with increasing frequency for all the evaluated temperatures.

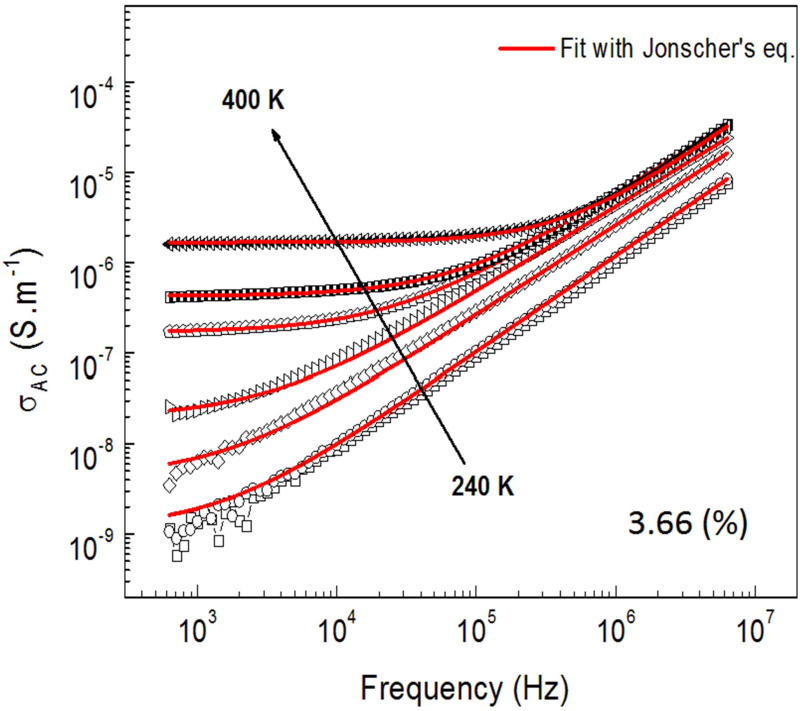

FIG. 5. Ac conductivity as a function of the frequency for various temperatures, for a concentration below the percolation threshold, 3.66 %. The solid curve represents the fitting according to the Jonscher's universal power law.

Fig. 6 reports the obtained results for $\phi \approx 6.21\,\%$; i.e., above the percolation threshold. It is also clear that the ac electrical conductivity is both frequency and temperature dependent. At low frequencies, σ_{ac} remains constant or tends to constant values, but it is strongly dependent on the temperature. The low-frequency plateau in σ_{ac} consists of the dc conductivity contribution. At higher frequencies, the conductivity becomes strongly frequency dependent and the origin of this behavior is related to the relaxation phenomena arising from mobile charge carriers [27]. The observed frequency dependence of the ac conductivity can be described by the Jonscher's universal power law [27-28].

$$\sigma_{ac}(\omega, T) = \sigma_{dc} + A.\omega^{S} \qquad (2)$$

where σ_{dc} is the frequency independent component of the ac conductivity, ω is the angular frequency, A is a temperature dependent parameter and the exponent s is interpreted as a measure of the degree of interaction between the charge carriers and the environment in their vicinity [29]. In general, the exponent s values are in the $0 \leq s \leq 1$ range. The experimental values of s, extracted using the Jonscher's power law in the σ_{ac} plots of the rGO/epoxy composites (at 300 K), for concentrations below and above percolation threshold, are reported in our previous work [10]. For samples above the percolation threshold, we can see that the temperature effect on the ac electrical conductivity shows a PTCR and NTCR effect below and above the glass transition temperature T_g, respectively. This can be clearly observed in Fig. 6, for 6.21 % of rGO, as an example. Three distinct regions are observed: below 350 K, where there is an increase of the ac electrical conductivity with increasing temperature (Fig. 6a), from 360 to 380 K (Fig. 6b), where an opposite behavior is observed, indicating the PTCR effect and finally, the results above 380 K (Fig. 6c) indicate an NTCR effect. A similar phenomenon has also been reported by K. Abazine et al. [16] for CNT/polyester composites below and above the glass transition temperature.

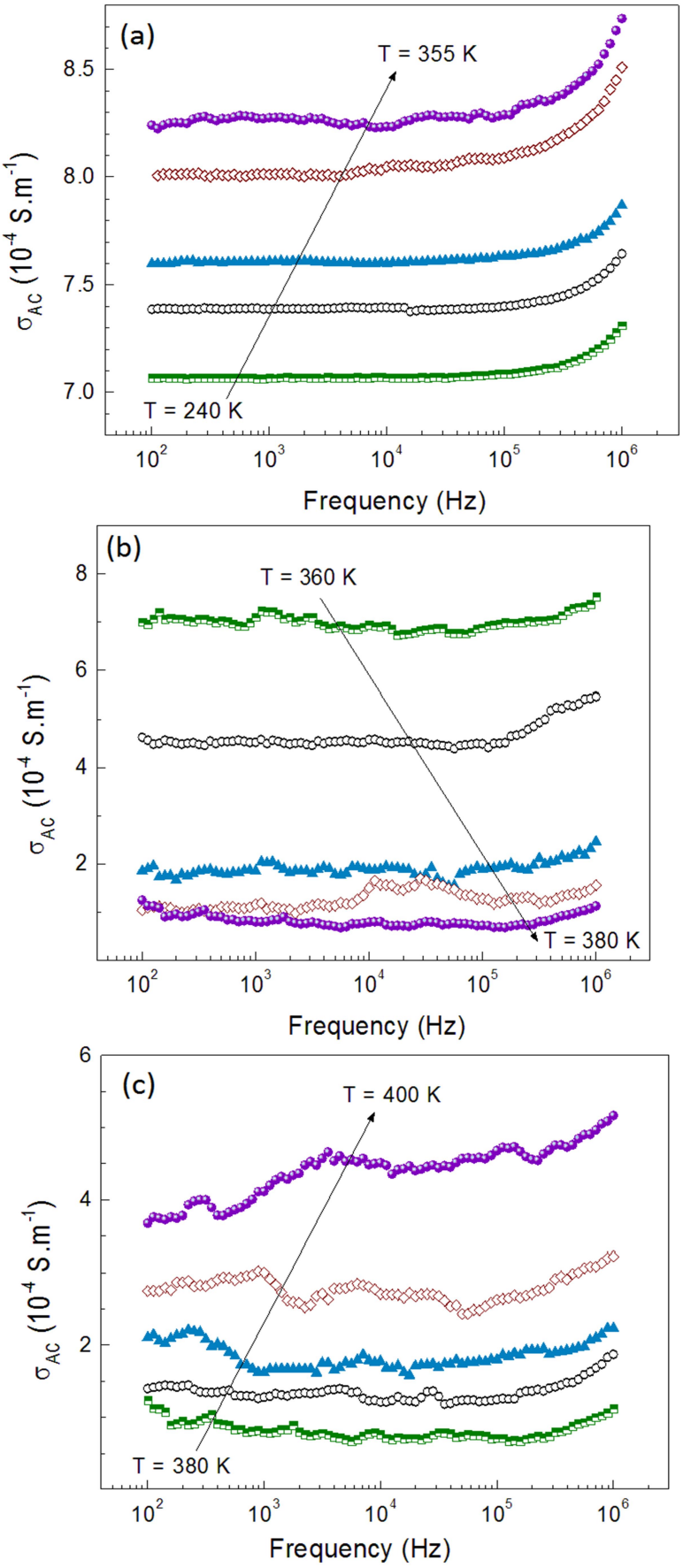

FIG. 6. Frequency dependence of the ac conductivity, σ_{ac} for a concentration above the percolation threshold, 6.21 %, for temperatures below and above the glass transition (T_g).

The experimental values of the s parameter are plotted in Fig. 7 for samples above the percolation threshold, where one can see that it is temperature dependent and we can identify the three distinct domains, for all samples. The typical value of s between 0 and 1 suggests ac conductivity through a hopping mechanism. The highest value of s describes a completely correlated system. In our case, the obtained value is low, which can be related to the effect of the distribution of relaxation path times and the degree of interaction between the charge carriers and the environment in their vicinity.

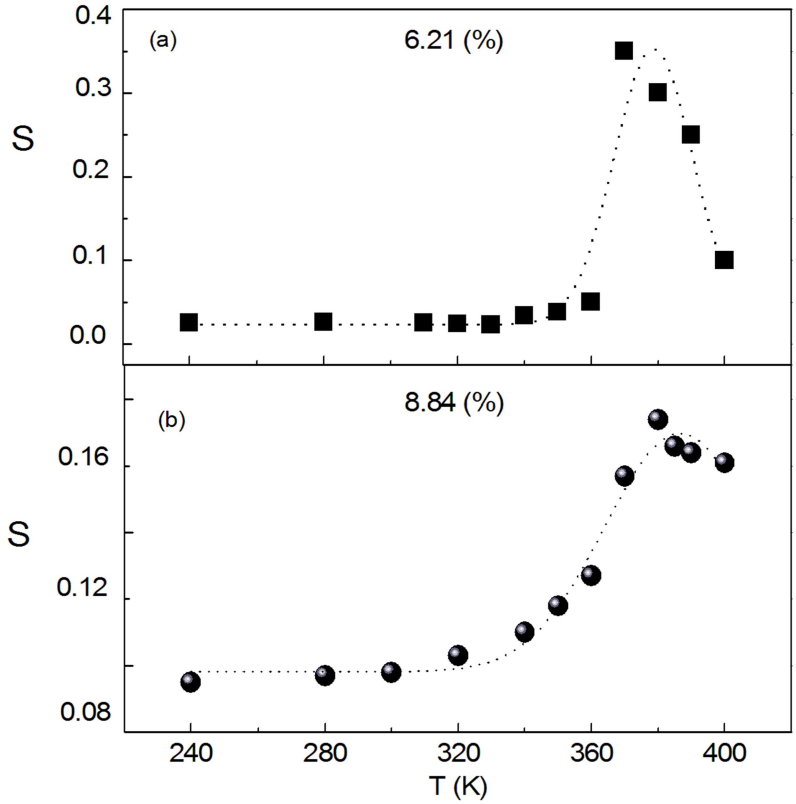

FIG. 7. Jonscher's exponent s *versus* temperature for concentrations above the percolation threshold, (a) 6.21 % and (b) 8.84 %.

In addition, Fig. 8 illustrates the $Ln(\sigma_{dc})$ dependence with the inverse of the temperature above $T_g \approx 360$ K, for composites with composition below and above the percolation threshold. Above the percolation threshold ϕ_C (Fig. 8b), a change in the slope of the ln (σ_{dc}) *versus* 1000/T plot, around T ≈ 380 K, is visible. As one can see, σ_{dc} increases exponentially with the temperature, indicating that the conductivity is thermally activated. The dependency was found to follow an Arrhenius behavior, as expressed by Eq. (3):

$$\sigma_{dc} = \sigma_0 . \exp(\frac{-E_a}{k_B . T}) \quad (3)$$

where σ_0 is a pre-exponential factor, E_a is the activation energy, k_B is the Boltzmann's constant and T is the temperature. The values of the activation energy for the various rGO concentrations below and above the percolation threshold were calculated and illustrated in Table 1.

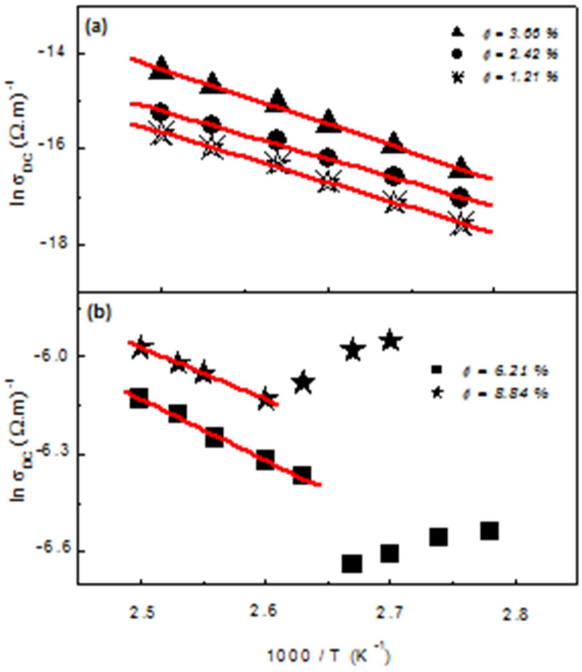

Fig. 8: Arrhenius plot of the dc conductivity *versus* 1000/T for concentrations of rGO particles below (a) and above (b) the percolation threshold. The solid lines are the least square linear fits to the Arrhenius relation.

Table 1. The activation energy for the various rGO concentrations below and above the percolation threshold $\phi_c \approx 4\%$, for the composite rGO/DGEBA.

Concentration (%)	1.21	2.42	3.66	6.21	8.48
E_a *(eV)*	1.02	0.93	0.88	0.08	0.015

As can be seen in this table, there is a decrease of the activation energy as the filler concentration increases; this behavior may be due to an increase of polarization energy and/or charge carrier density, leading to a decrease of the domain boundary potential of rGO into the epoxy polymer matrix.

Conclusion

We described the dc and ac electrical conductivities of percolative systems, synthesized by mixing rGO particles in an epoxy resin polymer, below and above the percolation threshold. The dc electrical conductivity is strongly dependent on the rGO content, indicating a percolating behavior with a percolation threshold around ≈ 4 %. This relatively high value can be explained by the shape of the rGO particles and their tendency for agglomeration in the polymer matrix. The temperature dependence of the electrical conductivity obeys the Arrhenius law and indicates that there is a negative temperature coefficient in resistivity (NTCR) for concentrations below the percolation threshold $\phi \leq \phi_C$. Above the percolation threshold, $\phi \geq \phi_C$, three regions are observed: below 350 K, there is an increase of the electrical conductivity with increasing temperature, from 360 to 380 K an opposite behavior is observed, indicating a positive temperature coefficient in resistivity (PTCR) effect and finally, above 380 K, the measurements indicate an NTCR effect. A comparison of the rGO/epoxy composites' PTCR effect with other different composites from our previous works indicates that the PTC intensity of the rGO/epoxy samples is significantly higher compared to those of the other polymeric materials. Finally, the ac electrical conductivity is both frequency and temperature dependent and follows the Jonscher's power law.

Acknowledgements

The authors acknowledge FCT-CNRST bilateral cooperation and FEDER by funds through the COMPETE 2020 Program and National Funds through FCT - Portuguese Foundation for Science and Technology under the project UID/CTM/50025/2013. Also B. Melo Acknowledges Fundacão para a Ciência e Tecnologia (FCT) for the PhD grant (SFRH/BD/117487/2016).

References

[1] Huang, Z.M., Zhang, Y.Z., Kotaki, M. and Ramakrishna, S., Compos. Sci. Technol., 63 (2003) 2223.

[2] Spitalsky, Z., Tasis, D., Papagelis, K. and Galiotis, C., Prog. Mater. Sci., 35 (2010) 357.

[3] Dang, Z.M., Wang, L., Yin, Y., Zhang, Q. and Lei, Q.Q., Adv. Mater., 19 (2007) 852.

[4] Novoselov, K.S., Geim, A.K., Morozov, S.V., Jiang, D., Zhang, Y., Dubonos, S.V., Grigorieva, I.V. and Firsov, A.A., Science, 306 (2004) 666.

[5] Dongrui, W., Xiaoman, Z., Zha, J.W., Zhao, J., Dang, Z. and Guo, H.H., Polymer, 54 (2013) 1916.

[6] Huang, X., Yin, Z., Wu, S., Qi, X., He, Q., Zhang, Q., Yan, Q., Boey, F. and Zhang, H., Small, 7 (14) (2011) 1876.

[7] Tapan, D.K. and Smita, P., Poly-Plastics Tech. Eng., 52 (2013) 319.

[8] Galpaya, D., Wang, M., Liu, M., Motta, N., Waclawik, E. and Yan, C., Graphene, 1 (2012) 30.

[9] Kuilla, T., Srivastava, S.K. and Bhowmick, A.K., J. Appl. Polym. Sci., 111 (2009) 635.

[10] Nioua, Y., El Bouazzaoui, S., Melo, B.M.G., Presas, P.R., Graca, M.P.F., Achour, M.E., Costa, L.C. and Brosseau, C., J. Mater. Sci., 52 (2017) 13790.

[11] Costa, L.C., Chakki, A., Achour, M.E. and Graca, M.P.F., Physica B, 406 (2011) 245.

[12] Jun-Wei, Z., Wei-Kang, L., Rui-Jin, L., Jinbo, B. and Zhi-Min, D., J. Mater. Chem. A, 1 (2013) 843.

[13] Min-Kang, S. and Soo, J.P., Bull. Korean Chem. Soc., 30 (2009) 1337.

[14] Shuaiguo, Z., Dandan, L., Pengfei, Z., Guojie, L., Kun, D., Guo, J., Guoqiang, Z., Chuntai, L., Changyu, S. and Zhanhu, G., J. Mater. Chem. C, 5 (2017) 8233.

[15] http://www.graphenea.com/collections/graphene-oxide/products/reduced-graphene-oxide-1-gram [accessed on 01 December 2016].

[16] Abazine, K., Anakiou, H., El Hasnaoui, M., Graça, M.P.F., Fonseca, M.A., Costa, L.C., Achour, M.E. and Oueriagli, A., J. Compos. Mater., 50 (2016) 3282.

[17] El Hasnaoui, M., Graça, M.P.F., Achour, M.E., Costa, L.C., Lahjomri, F., Outzourhit, A. and Oueriagli, A., J. Mater. Environ. Sci., 2 (2011) 1.

[18] Marsden, A.J., Papageorgiou, D.G., Valles, C., Liscio, A., Palermo, V., Bissett, M.A., Young, R.J. and Kinloch, I.A., 2D Materials, 5 (2018) 1.

[19] Costa, L.C., Henry, F., Valente, M.A., Mendiratta, S.K. and Sombra, A.S., Eur. Polym. J., 38 (2002) 1495.

[20] Kuilla, T., Bhadra, S., Yao, D., Kim, N.H., Bose, S. and Lee, J.H., Prog. Poly. Sci., 35 (2010) 1350.

[21] Singh, V., Progx. Mater. Sci., 56 (2011) 1178.

[22] Ma, P-C., Siddiqui, N.A. and Marom, G., Compos., Part A : Appl. Sci. Manuf., 41 (2010) 1345.

[23] Soo-Jin, P.H., Min-K, S. and Jae-Rock, L., Carbon Science, 2 (2001) 159.

[24] Costa, L.C. and Henry, F., J. Mater. Sci. Lett., 22 (2003) 699.

[25] Boukheir, S.A., Len, A., Füzi, J., Kenderesi, V., Achour, M.E., Éber, N., Costa, L.C., Oueriagli, A. and Outzourhit A., Polymer Composites, 50 (2017) 183.

[26] Jun-Wei, Z., Dong-Hong, W., Yu, Y., Yun-Hui, W., Robert, K., Lib, Y. and Zhi-Min, D., RSC. Adv., 7 (2017) 11338.

[27] Jonscher, A.K., J. Mater. Sci., 13 (1978) 553.

[28] Jonscher, A.K., Nature, 267 (1977) 673.

[29] Momin, H. K., Adv. Mat. Lett., 5 (2014) 384.